13th ewtec 2019 Proceedings of the 13th European Wave and Tidal Energy Conference 1-6 Sept 2019, Naples, Italy

Wake dynamics in a six-bladed horizontal axial turbine through a coupled DES-Actuator Lines Model

Jorge Sandoval, Cristián Escauriaza, and Clemente Gotelli

***Abstract*—This study presents a numerical investigation of the wake developed behind a six-bladed horizontal axis tidal turbine (Sabella D10 device) using a coupled model: the flow is solved through a Detached-Eddy Simulation (DES) model, whereas the turbine is represented in the flow through an Actuator-Lines Model (ALM). We focused on the most important turbulent structures of the wake induced by the turbine, where three main mechanisms could be clearly identified: (1) Unsteady tip vortices generation at the top of the blades that are shed downstream in helicoidal structures, (2) a local blade wake which is produced by the rotational movement of the actuator lines, and (3) a wake developed behind the hub. These structures interact as they move downstream, producing a resulting wake with complex hydrodynamics. This combined scheme can be carried out with relatively low computational cost, providing a consistent framework to study the impacts of marine hydrokinetic turbines (MHK) in natural tidal channels, as well as to improve the arrangements design and optimization of turbine arrays in realistic conditions.**

***Index Terms*—3D numerical models, Marine Hydrokinetic turbines, Actuator Lines Model, turbulent coherent structures.**

I. Introduction

THE interaction between Marine Hydrokinetic (MHK) devices and the flow developed in tidal channels produces turbulent wakes with complex hydrodynamics. These flows are characterized by the presence of large-scale coherent structures of different temporal and spatial scales with a high rotational component induced by the operation of the turbines. These interactions have an important influence on the surrounding environment in many key aspects, i.e. local flow conditions, sediment transport, ecosystem dynamics, submarine noise, among others. Furthermore, wake interactions among devices in turbine arrays play a significant role in energy extraction performance.

In order to study the complex phenomena associated to the wake dynamics and their implications, numerical simulations are a necessary tool to assess the effects of the flow, providing detailed information and supporting a wide range of application cases. In this context, three-dimensional (3D) numerical simulations of devices at high Reynolds numbers play a significant role on the understanding of the flow dynamics and physical impacts on the environment for real operation conditions and different arrays configurations. Moreover, this methodology offers very useful information about wake interactions among devices providing key insights for arrangement optimization. This study presents a numerical investigation of the wake developed behind a six-bladed horizontal axial turbine (Sabella D10 model) using a coupled approach: the flow is solved through a hybrid URANS/LES formulation known as Detached-Eddy Simulation (DES), whereas the turbine is represented through an Actuator-Lines Model (ALM).

The paper is organized as follows: In section II we describe the numerical model based on a hybrid formulation, which captures the large-scale turbulent coherent structures of the flow. Section III contains the study case and the model setup for simulations. In Section IV we present the results for simulations, analyzing the main structures induced by the turbine in the flow and the time-averaged flow field. In Section V we finally present the conclusions of this work and perspectives for future research.

Paper ID number:1750- Conference track: Tidal hydrodynamic modelling

J. Sandoval is with Marine Energy Research and Innovation Center (MERIC), Santiago, Chile (e-mail: jorge.sandoval@meric.cl).

C. Escauriaza is with Hydraulic and Environmental Engineering Department, Pontificia Universidad Católica de Chile, Santiago, CHILE and Marine Energy Research and Innovation Center, Santiago, Chile (e-mail: cescauri@ing.puc.cl).

C. Gotelli is with Marine Energy Research and Innovation Center (MERIC), Santiago, Chile (e-mail: clemente.gotelli@meric.cl).

II. Numerical simulations of flow-turbine interaction using a coherent structure-resolving turbulence model

The interaction between the flow and rotating axial turbines induces wakes with a highly three-dimensional flow dominated by dynamically-rich turbulent coherent structures. These flows can be described by turbulence models that capture both the time-averaged and instantaneous flow field through different approaches.

Statistical models based on URANS formulations can typically resolve certain features of shear-driven coherent structures, but despite they have been widely used and validated for tidal turbine applications, they model turbulence implicitly, being not capable of resolving the unsteady flow field in the wakes. On the other hand, models based on LES, which only dissipate turbulent features smaller than the grid resolution, can capture the rich dynamics of the wakes, but their computational cost at high-Reynolds numbers can increase significantly, especially when high resolution is required near solid boundaries [1], [2].

Hybrid URANS/LES turbulence models can improve these shortcomings, resolving the turbulent

coherent structures of the flow, using moderate computational costs, and providing a realistic approach for tackling these complex flows. In this work, we use detached-eddy simulations, a hybrid URANS/LES formulation [3], based on the one-equation eddy-viscosity turbulence model developed by Spalart and Allmaras [4]. In the following subsections, we describe the model for DES, which is coupled with an ALM for the representation of the turbines..

A. Numerical Model for DES

The governing equations used in our DES model are the incompressible 3D unsteady Reynolds-averaged equations for the conservation of mass and momentum.

$$\frac{\partial u_i}{\partial x_i} = 0 \tag{1}$$

$$\frac{\partial u_i}{\partial t} + \frac{\partial u_i u_j}{\partial x_j} = -\frac{\partial p}{\partial x_i} + \frac{1}{Re}\frac{\partial^2 u_i}{\partial x_j \partial x_j} - \frac{\partial}{\partial x_j}\langle u_i' u_j' \rangle + S_i \tag{2}$$

S_i is the momentum term obtained from the Actuator-Lines Model. This term corresponds to a density-normalized force that is imposed by the actuator points on the domain. The magnitude of the forces is computed using the local velocity obtained from DES and the local blades characteristics. The blade airfoil type, chord and twist, as well as lift and drag coefficients are obtained from a look-up table which are interpolated each time step.

For all the simulations presented in this work, we use the model, developed by Paik et al. [5] and Escauriaza & Sotiropoulos [2], which is second-order accurate in time and space, and parallelized with MPI libraries for computers with distributed memory.

Since the effects of ambient turbulence are key for the performance and wake development of tidal turbines [6], [7], we have incorporated into our model an unsteady turbulent inlet generator. Using a stochastic formulation, we feed the DES with an unsteady inlet profile, in which we can define the characteristic time and length scales of the incoming turbulence [8], [9]. These synthetic profiles satisfy continuity and approximate the potential anisotropic features in ambient turbulent flows.

Applications and performance of this model have been discussed in detail in a series of previous papers (e.g. Paik et al., [5], [10]; Escauriaza & Sotiropoulos [11], [12]; Link et al., [13]). In all these studies, the accuracy of the numerical method was demonstrated by qualitative and quantitative comparisons with available experimental data, typically in terms of mean flow quantities and turbulence statistics.

B. Actuator Lines Model

The Actuator-Lines Model represents the turbines as body forces in the flow equal and opposite to the lift and drag forces experienced by the turbine [14]. Each blade is represented as an actuator line and in turn, each actuator line is divided into several equally distributed segments represented by actuator points. To compute lift and drag forces we perform a geometrical decomposition as is shown in Fig 1:

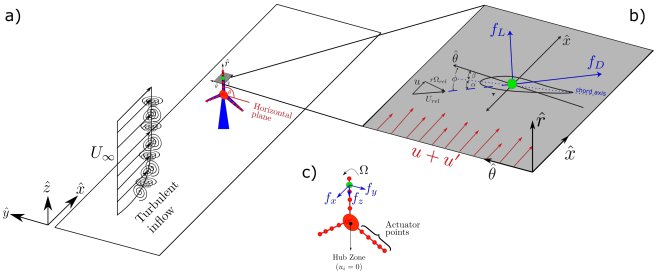

Fig. 1. Schematic representation of the ALM approach. The blade are represented by an finite number of equally-distributed actuator points (a). Each actuator point represents a blade section with known geometry and lift and drag coefficients (b). With the relative velocity, the angle of attack and the Reynolds number, the lift and drag coefficients are obtained from a look-up table and used to compute lift and drag forces. After filtering the forces by a Gaussian function, the forces are projected and incorporated on the 3D flow (c).

Each actuator point represents a blade section with known geometry (chord length and twist angle) and lift and drag coefficients (see figure 1.b). Depending on the relative velocity angle, the angle of attack is computed. With that information and the Reynolds number, the lift and drag coefficients are obtained from a look-up table and used to compute lift and drag forces. Finally, we filter the forces by a Gaussian function to smooth spurious velocity oscillations and project them on the 3D flow (see figure 1.c).

For an actuator point located at a radial distance r from the turbine center, the relative speed U_{rel} is calculated as:

$$U_{rel} = \sqrt{u^2 + (r\Omega_{rel})^2} \tag{3}$$

Where u is the local instantaneous streamwise velocity component and Ω_{rel} is the relative rotational speed between the blade and the fluid. The latter is written as:

$$\Omega_{rel} = r\Omega + v\sin\theta_b - w\cos\theta_b \tag{4}$$

Where θ_b is the azimuthal angle between an actuator point node of the b-blade (actuator line) and the horizontal plane as shown in Fig 1.a., v and w are the local transverse and vertical velocity components, respectively, and Ω is the turbine rotational speed, which is assumed constant.

In addition, the relative flow angle is obtained by

$$\phi = \tan^{-1}\left(\frac{u}{\Omega_{rel}\cdot r}\right) \tag{5}$$

We calculate the local angle of attack α by subtracting the local blade twist angle as follows (for details, see Fig 1.b),

$$\alpha = \phi - \beta \tag{6}$$

The lift and drag forces per span unit length on the blades are calculated as a function of the radial distance, the relative velocity, and the angle of attack such that,

$$\vec{f}_{2D} = (f_L, f_D) \tag{7}$$

$$(f_L, f_D) = \frac{1}{2}\rho U_{rel}^2 c(r)\left(C_L(\alpha, Re)\hat{L} + C_D(\alpha, Re)\hat{D}\right) \tag{8}$$

Where $\hat{L}$ and $\hat{D}$ are the local lift and drag directions for each actuator point. These forces are geometrically re-projected on 3D space before to be applied onto the flow (see Fig 1.c). To spread the forces in the space, we follow the methodology proposed by [14], where the force at a grid cell located at (x, y, z), is related to the actuator lines forces as follows:

$$\vec{f}(x, y, z) = \sum_{b=1}^{N_b} \int_{R_h}^{R} \vec{f}_{2D}(r_b)\eta_\epsilon(d)dr_b \tag{9}$$

Here, N_b is the number of blades, d is the distance between the point located at (x, y, z) and the actuator point of the b-blade located at r_b and η_ϵ is a Gaussian projection function defined as

$$\eta_\epsilon = \frac{1}{\epsilon^3 \pi^{3/2}} \exp\left(-\frac{d^2}{\epsilon^2}\right) \tag{10}$$

Where ϵ is the radius of the projection force and it is computed as $\epsilon = 2\sqrt{\Delta x \Delta y \Delta z}$ [15].

III. Study Case and Model Setup

In this work, we used the DES-ALM to study the D10 Sabella turbine model of a laboratory-scaled case performed by Gotelli et al [15]. The scale used for the experiments is 1:108 and all the instantaneous velocity data obtained on this measurements was filtered using the spikes removal technique proposed by [16]. For the simulations, we used a rectangular mesh of 9.3 million nodes, which are clustered near the solid wall using a hyperbolic tangent distribution, with $y^+ > 1.0$. The grid is also clustered in the zone where the turbine is located to get a better capture of the interaction between the flow and the device (see Figure 2). The velocity scale used was the upstream velocity, whereas the length scale selected was the water depth.

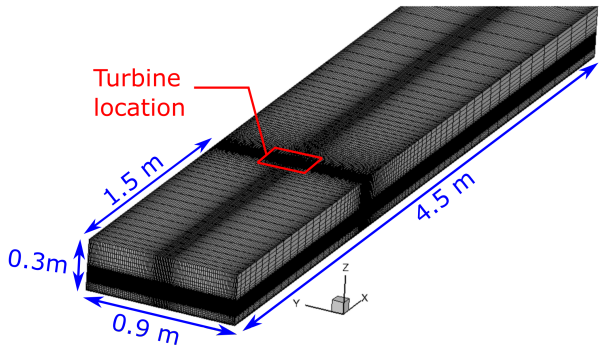

Fig. 2. Grid used for simulations. For a better representation, in every direction, only one every three nodes are shown.

The studied device correspond to a six-bladed turbine with elliptical foil geometry. Main turbine parameters and hydrodynamic conditions for this study case are presented in Table 1.

TABLE I
Principal Turbine and Flow Parameters for the Studied Case

Parameter	Definition	Value
D	Diameter	0.092 m
D_h	Hub diameter	0.036 m
h_h	Hub height	0.1 m
N_b	Number of blades	3
h_w	Water depth	0.3 m
b_f	flume width	0.9 m
Re	Reynolds number	126667
Fr	Froude number	0.24
U_∞	Upstream velocity	0.42 m/s
Ω	Rotor angular velocity	16.6 rad/s
TSR	Tip-speed ratio	3.65

For the inlet boundary condition, we used the random flow generator technique proposed by Smirnov et al. [8] which is capable to reproduce the ambient turbulence intensity ($\sim$ 10%) . Through this technique, an instantaneous velocity field is incorporated at the inlet each time step, which preserve the turbulent features of the flow used to generate it [1]. No-slip conditions are imposed at all solid boundaries, while a zero-shear and rigid plane boundary condition is applied at the free surface. Finally, for the outlet a characteristics-based non-reflecting boundary condition is applied. This approach allows the vortical structures to exit the domain without distorsions [17].

IV. Results

Through numerical simulations, we investigated the physical mechanisms involved in the interaction between the turbulent flow and the MHK device. Particularly, we focused on the most important structures of the wake induced by the turbine, where three main mechanisms could be clearly identified: (1) Unsteady tip vortices generation at the top of the blades that are shed downstream in helicoidal structures, (2) a local blade wake which is produced by the rotational movement of the actuator lines, and (3) a wake developed behind the hub. These structures interact as they move downstream, producing a resulting wake with complex hydrodynamics (see Fig 3).

In the case of tip-vortices, these structures move downstream until the flow becomes unstable, where they breakup and mix with the rest of the wake structures. This phenomenon can be more comprehensively observed in Fig 4, where a peak zone of turbulent kinetic energy is visualized at the location where the breakup is produced. This mechanisms has been reported in other studies ([18], [19], [20]) and has been established as a process that enhances the turbulence and the wake expansion.

In Fig 5.a., we show the time-average streamwise velocity field for a central vertical plane. In the figure, we can see that the near wake region presents a strong velocity deficit induced by the hub. Nevertheless, for

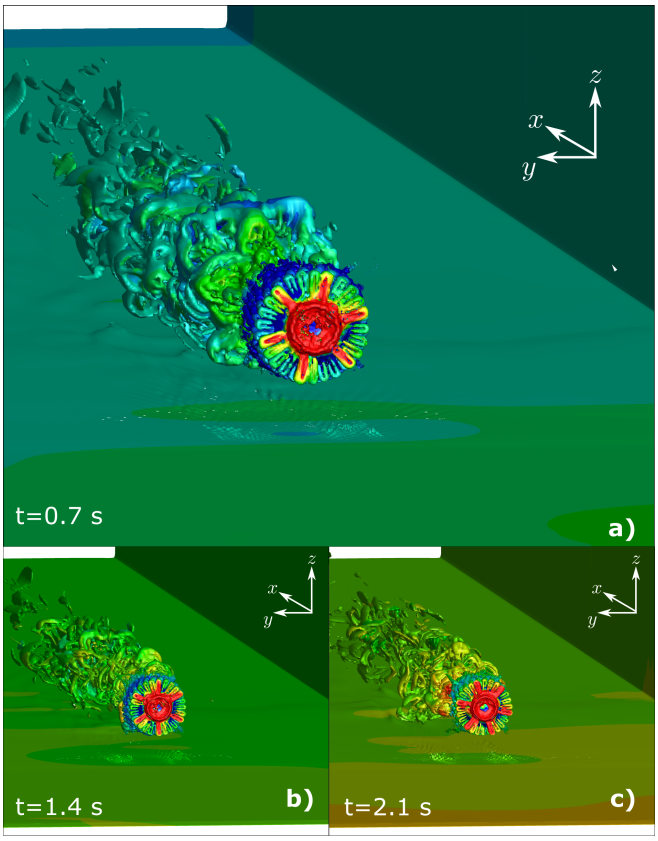

Fig. 3. a) – c) Instantaneous vorticity magnitude iso-surfaces at different times.

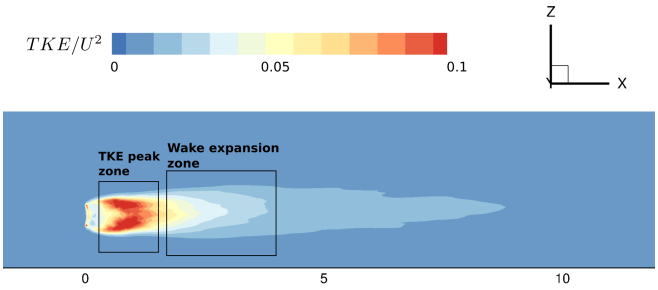

Fig. 4. Turbulent kinetic energy magnitude field on a vertical plane at the center of the turbine

turbines with high radial aspect ratio (D/D_h) the streamwise velocity deficit represents a problem in the model due to the lack of physical representation of the local hydrodynamics (the hub zone is represented as a zone with zero velocity). In Fig 5.b. we plot the comparison between the experimental measurements at centerline ($z = h_h$, behind the turbine) and the model. The results show that the model underestimate the velocity deficit.

V. Conclusion

An Actuator Lines Model was coupled with a coherent-structure resolving DES model. This combined approach allowed us to capture some important features of the rotational dynamics of the interaction between the turbulent flow and the device, as well as the complex coherent-structure dynamics of the wake.

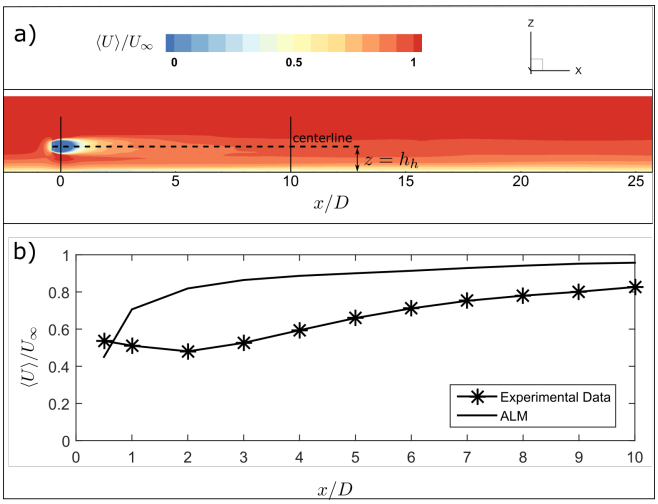

Fig. 5. a) Non-dimensional time-averaged streamwise velocity field at a vertical plane in the center of the flume. b) Non-dimensional time-averaged streamwise velocity at centerline ($z = h_h$)

Despite the instantaneous flow field show a good representation of the main structures of the wake, the time-averaged flow showed an underestimation of the velocity deficit behind the turbine due to the over-simplification of the hub effects on the flow in the model. It suggests the importance of a better formulation of the hydrodynamical effects of the hub in the flow, especially in devices with a high radial aspect ratio (where the hub effects could be significant).

In future work, we will improve the geometry representation of the turbine in our simulations using the overset grid approach. This will allow us to capture both, the near and far wake hydrodynamics of the interaction and the local effects of the supporting structure in the flow.

Acknowledgement

This work has been supported by the Marine Energy Research & Innovation Center (MERIC) project, CORFO 14CEI2-28228. Powered@NLHPC: This research was partially supported by the supercomputing infrastructure of the NLHPC (ECM-02).

References

[1] D. Gajardo, C. Escauriaza, and D. M. Ingram, "Capturing the development and interactions of wakes in tidal turbine arrays using a coupled bem-des model," *Ocean Engineering*, vol. 181, pp. 71–88, 2019.

[2] C. Escauriaza and F. Sotiropoulos, "Lagrangian model of bed-load transport in turbulent junction flows," *Journal of Fluid Mechanics*, vol. 666, p. 36–76, 2011.

[3] P. R. Spalart, "Detached-eddy simulation," *Annual Review of Fluid Mechanics*, vol. 41, no. 1, pp. 181–202, 2009. [Online]. Available: https://doi.org/10.1146/annurev.fluid.010908.165130

[4] P. Spalart and S. Allmaras, "A one-equation turbulence model for aerodynamic flows," *AIAA*, vol. 439, 01 1992.

[5] J. Paik, C. Escauriaza, and F. Sotiropoulos, "On the bimodal dynamics of the turbulent horseshoe vortex system in a wing-body junction," *Physics of Fluids*, vol. 19, no. 4, p. 045107, 2007. [Online]. Available: https://doi.org/10.1063/1.2716813

[6] T. P. Lloyd, S. R. Turnock, and V. F. Humphrey, "Assessing the influence of inflow turbulence on noise and performance of a tidal turbine using large eddy simulations," *Renewable Energy*,

vol. 71, pp. 742 – 754, 2014. [Online]. Available: http://www.sciencedirect.com/science/article/pii/S0960148114003516

[7] T. Blackmore, W. Batten, and A. Bahaj, "Influence of turbulence on the wake of a marine current turbine simulator," *Proceedings of the Royal Society A: Mathematical, Physical and Engineering Sciences*, vol. 470, no. 2170, p. 20140331, 2014.

[8] A. Smirnov, S. Shi, and I. Celik, "Random flow generation technique for large eddy simulations and particle-dynamics modeling," *Journal of fluids engineering*, vol. 123, no. 2, pp. 359–371, 2001.

[9] R. Laraufie, S. Deck, and P. Sagaut, "A dynamic forcing method for unsteady turbulent inflow conditions," *Journal of Computational Physics*, vol. 230, no. 23, pp. 8647 – 8663, 2011. [Online]. Available: http://www.sciencedirect.com/science/article/pii/S0021999111004840

[10] J. Paik, C. Escauriaza, and F. Sotiropoulos, "Coherent structure dynamics in turbulent flows past in-stream structures: Some insights gained via numerical simulation," *Journal of Hydraulic Engineering*, vol. 136, no. 12, pp. 981–993, 2010.

[11] C. Escauriaza and F. Sotiropoulos, "Reynolds number effects on the coherent dynamics of the turbulent horseshoe vortex system," *Flow, Turbulence and Combustion*, vol. 86, no. 2, pp. 231–262, Mar 2011. [Online]. Available: https://doi.org/10.1007/s10494-010-9315-y

[12] ——, "Initial stages of erosion and bed form development in a turbulent flow around a cylindrical pier," *Journal of Geophysical Research: Earth Surface*, vol. 116, no. F3, 2011.

[13] O. Link, C. González, M. Maldonado, and C. Escauriaza, "Coherent structure dynamics and sediment particle motion around a cylindrical pier in developing scour holes," *Acta Geophysica*, vol. 60, no. 6, pp. 1689–1719, Dec 2012. [Online]. Available: https://doi.org/10.2478/s11600-012-0068-y

[14] J. N. Sørensen and W. Z. Shen, "Numerical modeling of wind turbine wakes," *Journal of fluids engineering*, vol. 124, no. 2, pp. 393–399, 2002.

[15] C. Gotelli, M. Musa, M. Guala, and E. Cristian, "Experimental and numerical investigation of wake interactions of marine hydrokinetic turbines," *Energy (submitted)*, 2018.

[16] M. Parsheh, F. Sotiropoulos, and F. Porté-Agel, "Estimation of power spectra of acoustic-doppler velocimetry data contaminated with intermittent spikes," *Journal of Hydraulic Engineering*, vol. 136, no. 6, pp. 368–378, 2010.

[17] C. Escauriaza, "Three-dimensional unsteady modeling of clear-water scour in the vicinity of hydraulic structures: Lagrangian and eulerian perspectives. retrieved from the university of minnesota digital conservancy, http://hdl.handle.net/11299/60294." 2008.

[18] D. Foti, X. Yang, M. Guala, and F. Sotiropoulos, "Wake meandering statistics of a model wind turbine: Insights gained by large eddy simulations," *Physical Review Fluids*, vol. 1, no. 4, p. 044407, 2016.

[19] S. Kang, X. Yang, and F. Sotiropoulos, "On the onset of wake meandering for an axial flow turbine in a turbulent open channel flow," *Journal of Fluid Mechanics*, vol. 744, pp. 376–403, 2014.

[20] P. Lyu, W.-L. Chen, H. Li, and L. Shen, "A numerical study on the development of self-similarity in a wind turbine wake using an improved pseudo-spectral large-eddy simulation solver," *Energies*, vol. 12, no. 4, 2019. [Online]. Available: http://www.mdpi.com/1996-1073/12/4/643